VSP

Journal of Biomaterials Science 23 (2012) 43–61

Journal of BIOMATERIALS SCIENCE
brill.nl/jbs

Properties of Antibacterial Polypropylene/Nanometal Composite Fibers

S. M. Gawish [a], **H. Avci** [b], **A. M. Ramadan** [a], **S. Mosleh** [a], **R. Monticello** [c], **F. Breidt** [d] **and R. Kotek** [b,*]

[a] National Research Center, Textile Research Division, Dokki, Cairo, Egypt

[b] College of Textiles, Textile Engineering Chemistry and Science, North Carolina State University, Raleigh, NC 27695-8301, USA

[c] AEGIS Environments 2205 Ridgewood Drive, Midland, MI 48642-5884, USA

[d] Department of Food Science, North Carolina State University, Raleigh, NC 27695, USA

Received 10 August 2010; accepted 2 November 2010

Abstract

Melt spinning of polypropylene fibers containing silver and zinc nanoparticles was investigated. The nanometals were generally uniformly dispersed in polypropylene, but aggregation of these materials was observed on fiber surface and in fiber cross-sections. The mechanical properties of the resulted composite fibers with low concentration of nanometal were comparable to those for the control PP yarns. Extruded composite fibers that contained 0.72% silver and 0.60% zinc nanoparticles had outstanding antibacterial efficacy as documented by the percentage count reduction growth of *Escherichia coli* and *Staphylococcus aureus*. Fibers containing silver particles had improved antistatic properties.

Keywords

Isotactic polypropylene, silver nanoparticles, zinc nanoparticles, melt spinning, antibacterial efficacy, antistatic properties

1. Introduction

Polypropylene (PP) fiber is one of the most widely used synthetic fibers, because it is relatively inexpensive and has outstanding mechanical properties. On the other hand, silver nanoparticles are unique, possessing high thermal stability and little toxicity to mammalian cells and tissues. Products made from PP/nanometals materials should have resistance to bacteria or pathogenic fungi and as a result could be used for hygienic and medical uses [1–6], such as surgical masks, diapers, filters, burn and wound dressings, hygienic bands, as well as other applications such

* To whom correspondence should be addressed. E-mail: rkotek@ncsu.edu

 DOI:10.1163/092050610X541944

as carpets, automotive parts, underwear, socks, technical textiles, athletic and military fabrics. Metal nano- or microparticles can be incorporated into PP by using the melt-spinning technique. Silver nanometals are non-toxic, inorganic additives and do not cause skin irritation. Also, they are bactericidal agents because they combine with the cellular protein of a broad spectrum of harmful microorganisms and inactivate them. High concentrations of metal salts coagulate cytoplasm proteins, resulting in damage of the cellular metabolism and the destruction of a microorganism.

A literature review revealed that Jeong *et al.* [1] used a conventional twin screw mixer to study the effect of additives and particle size of micro- and nano-sized silver powders on the antibacterial properties of PP/Ag fibers. The analysis and characterization of the compounds were done by X-ray diffraction, DSC, SEM, and by measuring mechanical properties and antibacterial activity. The authors concluded that fibers containing silver nanoparticles exhibited superior antibacterial activity compared to samples containing micro-sized particles. The same authors prepared nano-composite PP/Ag fibers to create permanent antibacterial effects [7] using a conjugate (bicomponent) spinning machine. Antibacterial efficiency against *Staphylococcus aureus* and *Klebsiella pneumonia* was excellent when the master batch was used as the sheath and not as the core of the fibers.

Dastjerdi *et al.* [8] have investigated the properties of bioactive continuous PP filament yarns containing Ag/TiO_2 nanocomposites. The processing of the starting materials and the characteristics and microbiological activities of the resulting fabric was studied. Variation in a nanofiller content improved tenacity and modulus of as-spun and textured fibers. Biostatic efficiency had no distinct trend with increasing silver content. Optimum antibacterial activity was shown for 0.75% nanofiller, which corresponded to the minimum degree of crystallinity for that sample.

The effect of various pigment additives on the fine structure of PP fibers was conducted by Broda *et al.* [9]. Studies on PP composite filaments with a reinforced nanoclay [10] and the effect of filler concentration on the mechanical and thermal properties of reinforced PP composite fibers were also determined [11]. Chae *et al.* [12] determined the effects of silver nanoparticles on the dynamic crystallization and also the physical properties of syndiotactic polypropylene. Previous research work was done by Kotek and co-workers [13, 14] at NCSU to study the mechanical and structural properties of melt-spun PP/nylon 6 alloy filaments as well as those of poly(trimethylene terephthalate) (PTT) filaments containing silver. The article showed that PTT fibers containing sufficient amounts of silver ions were effective in reducing *Escherichia coli*. Incorporation of silver sulfadiazine into PTT was not effective. The mechanical and antimicrobial properties of spun fibers were reported.

The present paper aims at studying the melt spinning of PP/nanometals composite fibers, especially new PP/Zn biocidal composite fibers which were produced and compared to PP/Ag fibers. These fibers were drawn fibers having permanent antibacterial and antistatic properties. They were prepared by using metal nanoparticles and melt spinning techniques. For this purpose, selected parameters were

chosen to attain the desired properties and maintain the bulk characteristic properties of the produced fibers. Such parameters included selecting a specific type of nanometal and also a low effective additive concentration. Mechanical properties of the composite fibers including tensile strength, elongation at break, modulus and tenacity were evaluated. The antibacterial activity of the composite Ag and Zn fibers was compared to the control PP fibers against *E. coli* and *S. aureus.* Surface morphology, antistatic and thermal properties of these fibers are also reported.

2. Materials and Methods

2.1. Materials

Isotactic polypropylene chips (PP 3155) were supplied by Exxon Mobil™. The polymer had a specific gravity of 0.902. Silver nanopowder ($d < 100$ nm, 99.5% metal, MW 107.87, mp 962°C), zinc nanopowder ($d < 50$ nm, 99% metal, MW 66.37, mp 419°C, density 7.14 g/cm^3, bp 908°C) and silver exchanged zeolite (granular 20 mesh) were supplied by Aldrich. A nonionic dispersing agent (polyethylene glycol monooleate, 100%) was obtained from Boehme Filatex Boehmelev NT.

2.2. Spinning Process

The machine used for research (Fig. 1) was a Hills bicomponent equipment containing double screw melt extruders (D-37007, 2002). Mixing of isotactic polypropy-

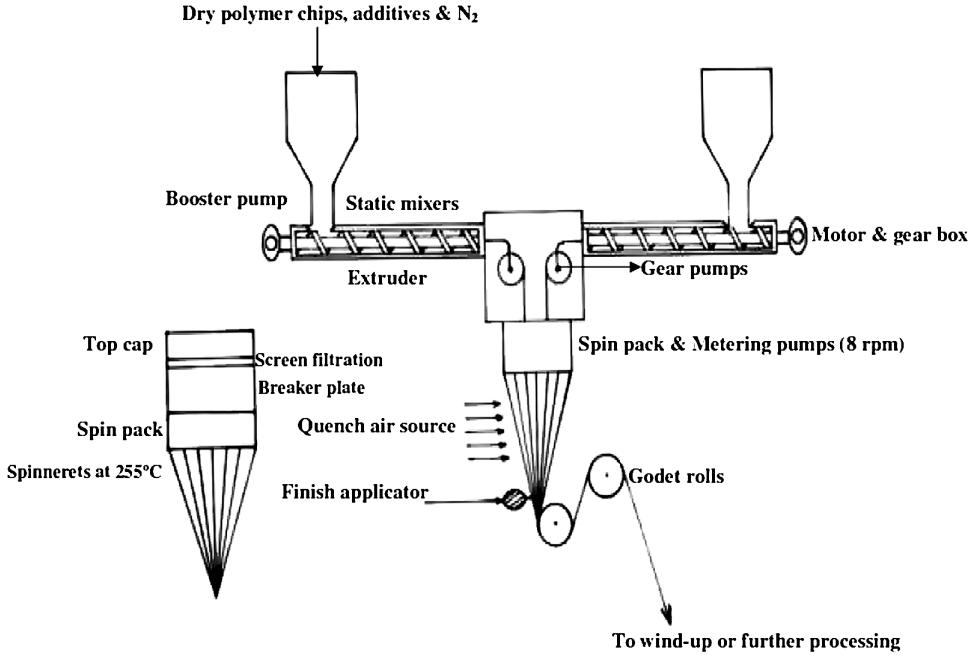

Figure 1. Bicomponent melt spinning machine.

lene (PP) chips and additives (silver and zinc nanopowders and 2 g/kg nonionic surfactant) was done first in a round 500 ml glass flask heated in a vacuum oven at 70°C for 1 h. The mix was then added with PP into the hoppers tanks under nitrogen gas. The melt was extruded through an automatic pressure control booster pump at a constant 8 rpm rate and was then metered with geared pumps. The extrusion process was conducted at 400 psi with a screw extruder length-to-diameter ratio of 24:1 and three static mixers with gradient temperatures. The first extruder zone was set at 220°C; the second one at 230°C and the third zone at 240°C. The second extruder was set at the same zone temperatures. A spin pack was designed for multifilament spinning yarns (288 filaments/yarn) and was equipped with mesh filtration screens. The round orifice of the spinneret was 0.6 mm in diameter and 1.38 mm in length. The multifilament yarn was cooled to room temperature and treated with Lurol PP, L 425 lubricant (Goulston Chemical) prior to drawing at 800 m/min or less at a draw ratio of up to 4.0. The final denier was 400.

2.3. Thermal Properties

A compensated differential scanning colorimeter (DSC Perkin-Elmer Model 7) equipped with a cooler was used under nitrogen flow. All samples were heated from 25 to 200°C at 20°C/min. Onset melting temperature was obtained from the intercept of the baseline and the maximum tangent of the corresponding exothermic and endothermic peaks. From the DSC graphs, melting temperatures (T_m) of the nanocomposite fibers were obtained and the apparent fusion enthalpies were calculated from the area of the endothermic peak. The degree of crystallinity of polypropylene was evaluated using the following equation:

$$X = \frac{\Delta H_f}{\Delta H_f^o} 100\%, \tag{1}$$

where X is the degree of crystallinity, ΔH_f the enthalpy heat of fusion of PP fibers and ΔH_f^o the enthalpy heat of fusion of 100% crystalline PP taken as 209 J/g [15, 16].

2.4. Mechanical Properties

The fiber count number (denier) was calculated at NCSU testing laboratory by the skein method according to ASTMD-1907 after conditioning the fibers at 20°C and 65% RH for 24 h. The strain at break, fiber modulus and tenacity were determined according to ASTM-D2256.

2.5. SEM Observations

Melt-spun fibers samples were coated with platinum under vacuum for 5 min and their cross-sections were observed under a scanning electron microscope (SEM, FE1Phenom) which was measured at 5 kV and up to 20 000× magnification, and also by using a field emission scanning electron microscope (FESEM, JEOL JSM-6340F).

2.6. TEM Observations

Bright-field TEM images were acquired using a JEOL 2000FX microscope operating at 200 kV. The thickness of the cross-sections was 110 nm. They were not coated. The particle size was determined by measuring the longest distance between the edges of a chosen particle.

2.7. Antibacterial Analysis

A modified AATCC 100 test method was adopted for measuring the antimicrobial activity of PP/metal composite fibers [17]. Two strains of bacteria, *E. coli* and *S. aureus*, were used. One piece of fiber string (20 cm; 0.31 mg) was placed in a 1.5 ml microcentrifuge tube; then 200 µl of saline containing 10^7 CFU/ml (log 7) of the organism was added to the tube, completely covering the fiber. This was incubated for 24 h at the appropriate temperature for the inoculated culture. After 24 h, LBG or YM plates were spread with the supernatant using a spiral platter (Model 4000, Spiral Biotech). After bacterial incubation at 37°C, colonies were counted. Plate counts were determined by an automatic spiral plate reader (Q count, Spiral Biotech). The reduction in bacteria growth count was calculated and compared to PP control (without any additive) as follows:

$$\text{Reduction of bacteria } (\%) = ((A - B)/A) \times 100, \tag{2}$$

where A is the initial number of bacterial colonies and B the final number of bacterial colonies after treatment with a PP/nanometal composite fiber.

2.8. Determination of Silver and Zinc Content

Fibers were cut into small pieces with stainless steel scissors, weighed with accuracy of 0.00001 g, placed into a Pyrex beaker, and then combusted in a muffle furnace with slowly raising the temperature by 100°C every 30 min and a final combustion to 550°C for 1 h. The residue was dissolved in 10 ml HNO_3 and filled with distilled water to 100 ml in a volumetric flask, rinsed several times with deionized water and then brought to volume. The solution was diluted 10 times and analyzed [17] on a Varian 820 ICP Mass Spectrometer to measure silver or zinc content in the solution.

2.9. Antistatic Tests

Tests were performed [18, 19] using a linear tester instrument (Fig. 2). Yarns were conditioned at 21°C and 43% RH for 24 h. Linear tester instrument is suitable for static charge measurements at low humidities. No static charges are generally observed for nylon 6 or 66 yarns under the textile standard conditions of 65% RH.

The static charge instrument involves two potential probes and one stainless steel friction pin. The first probe is located 3.5 cm from the pin (Fig. 3) and the second one is 41 cm from the first pin (Fig. 4). The fiber runs against the friction stainless steel pin and then is wound in front of the potential probe. The probe records the potential charge of the fiber with the potential detected on the two probes at a data

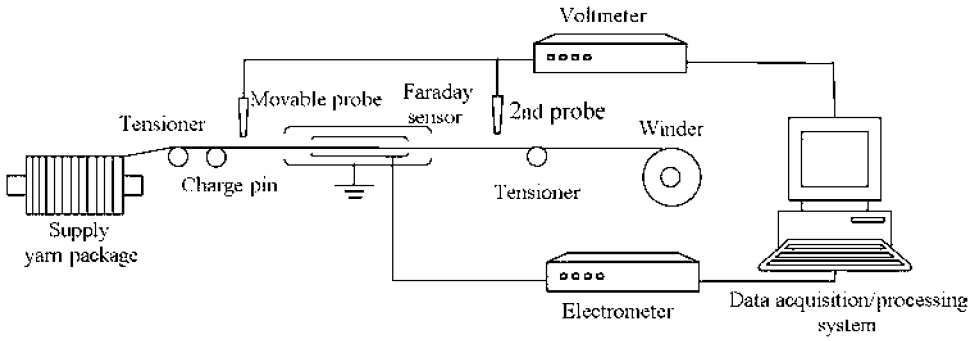

Figure 2. Linear tester instrument for static charges measurement.

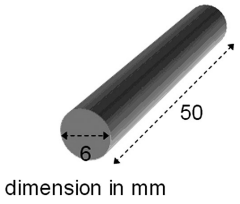

Figure 3. Stainless steel pin.

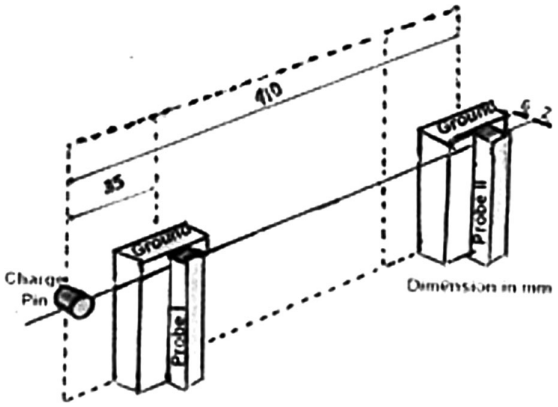

Figure 4. Charge in and probes.

collection rate of 100 data/s. The characteristic decay time and the initial generated potential at the fiber/pin separation point is calculated according to equation (3):

$$V = V_0 e^{-t/t^*}, \tag{3}$$

where V (in V) is the amount of electrostatic potential on the yarn surface after time t (in s) from the beginning of initial charge, V_0 (V) the electrostatic potential at the point of separation (initial charge potential at $t = 0$ s) and t^* (s) the characteristic decay time of the yarn under test conditions.

The rollers and all system guides were cleaned with alcohol before each experiment because any contamination significantly affects the static charge and decay time. The fiber winding speed was set at 40 m/min, and fiber tension was adjusted at 40 g for PP based on their dissipation factors to support the fiber on the instrument.

3. Results and Discussion

3.1. Yarn Thermal Properties

In order to compare the control sample with the composite, fibers containing zinc silver nanoparticles and also silver zeolite were used to determine thermal properties. DSC thermograms for all the filaments are shown in Figs 5–9. Table 1 gives

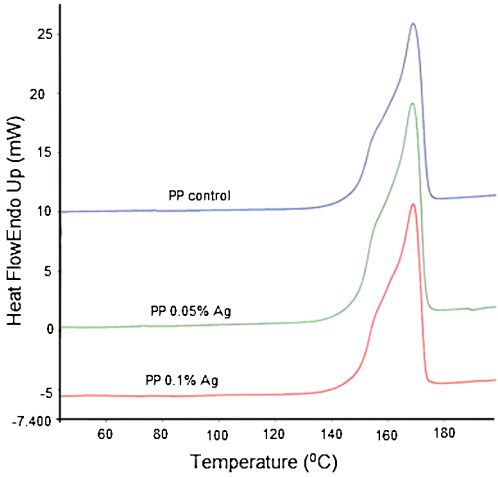

Figure 5. DSC heating curves for PP and PP/Ag composite fibers at a low silver concentration. This figure is published in colour in the online edition of this journal, which can be accessed *via* http://www.brill.nl/jbs

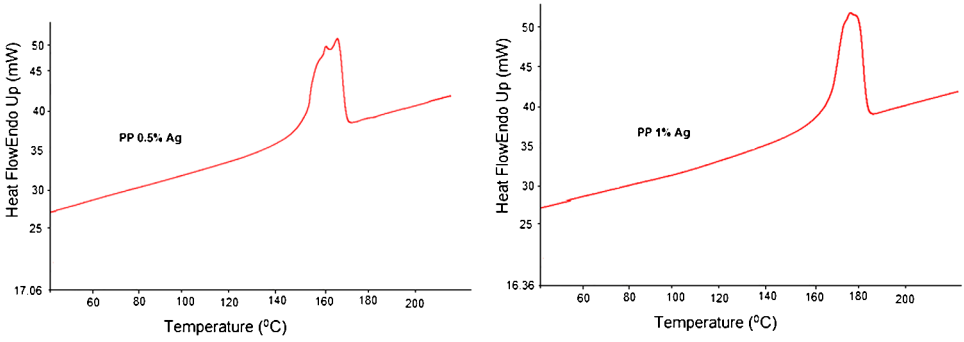

Figure 6. DSC heating curves for PP/Ag composite fibers with 0.5 and 1.0% silver content. This figure is published in colour in the online edition of this journal, which can be accessed *via* http://www.brill.nl/jbs

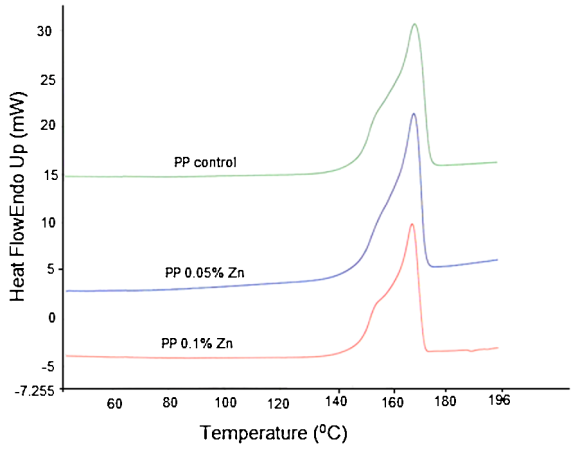

Figure 7. DSC curves for PP and PP/Zn composite fibers at a low concentration of zinc. This figure is published in colour in the online edition of this journal, which can be accessed *via* http://www.brill.nl/jbs

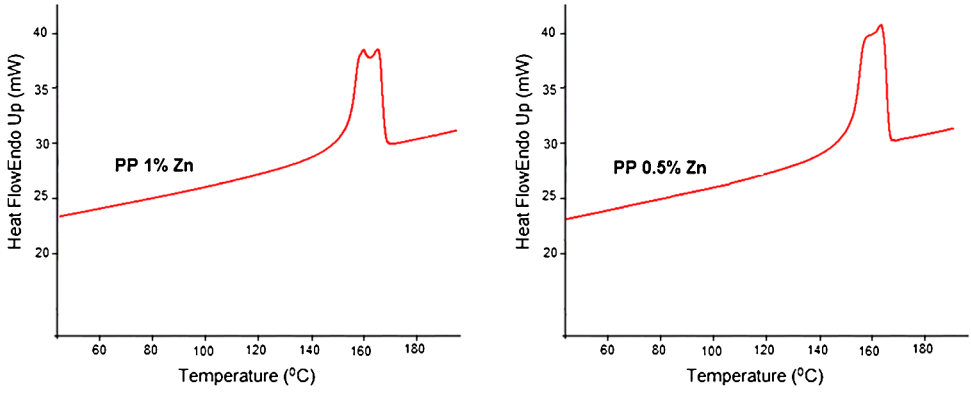

Figure 8. DSC curves for PP/Zn composite fibers with 0.5 and 1.0% zinc. This figure is published in colour in the online edition of this journal, which can be accessed *via* http://www.brill.nl/jbs

a summary of the melting points, the heat of fusion and the degree of crystallinity of the samples. There was a negligible change of the melting point of PP filaments with an increase in nanosilver content from 0.05 to 0.1%; however, the melting point slightly decreased when the silver content increased from 0.5 to 1%. PP/0.5% Ag yarn had the highest degree of crystallinity of 44.7%, but this value is still very close to that of 42.8% for the control sample. The similar crystallinity variation in was also observed by Yeong *et al.* [1].

Crystallization behavior is dependent on the cooling rate and the concentration of nanoparticles [1, 20–22]. At a high cooling rate of 20°C/min and a low nanosilver concentration, the particles did not act as nucleating agents in the polymer matrix and a marginal decrease in crystallinity is observed. On the other side, the silver par-

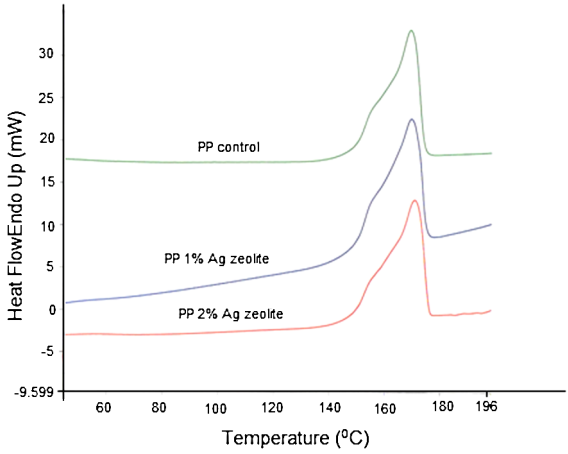

Figure 9. DSC curves for PP and PP/Ag zeolite composite fibers. This figure is published in colour in the online edition of this journal, which can be accessed *via* http://www.brill.nl/jbs

Table 1.
Thermal properties of PP composite fibers

Sample	Onset of melting point (°C)	Peak melting point (°C)	ΔH_f^o (J/g)	Degree of crystallinity (%)
PP control	157.3	169.1	89.5	42.8
PP/0.05% Ag	156.3	168.8	86.1	41.2
PP/0.1% Ag	156.8	168.9	85.6	40.9
PP/0.5% Ag	153.2	166.5	93.5	44.7
PP/1% Ag	152.9	160.7	87.0	41.6
PP/0.05% Zn	158.0	168.5	86.4	41.4
PP/0.1% Zn	158.2	167.7	87.4	41.8
PP/0.5% Zn	154.0	164.5	81.6	39.0
PP/1% Zn	154.6	159.8	80.4	38.5
PP/1% Ag zeolite	158.9	169.4	90.2	43.2
PP/2% Ag zeolite	157.9	170.7	85.5	40.9

ticles could act as heterogenous nucleating sites and facilitate crystallization growth at low cooling rate (5°C/min), depending on the concentration of the nanoparticles. Yeo *et al.* [2] proposed that silver can sometimes function as a nucleating agent and accelerate crystallization of PP.

Interestingly, the T_m values of fibers with a low content of zinc nanoparticles of 0.1% or less were close to that of the control (Table 1). A slight decrease of T_m was also observed for the PP filaments with the zinc content of 0.5 and 1%. A higher content of zinc nanoparticles could lead to a more dominant decrease of the melting point and the degree of crystallinity. Metal nanoparticles have a high thermal conductivity compared to PP as a non-polar polymeric matrix. Therefore, these

Table 2.
Mechanical properties of PP silver composite fibers

Sample	Denier	Strain-at-break (%)	Fiber modulus (gf/denier)	Fiber tenacity (gf/denier)	SD for fiber tenacity (gf/denier)
PP control	410	68.3	34.6	3.65	0.26
PP/0.025% Ag	407	70.4	31	3.80	0.18
PP/0.05% Ag	404	64.0	31.3	3.6	0.23
PP/0.1% Ag	410	67.1	32.4	3.7	0.37
PP/1% Ag zeolite	289	65.1	31.4	4.0	0.12

particles probably accelerated the quenching rate, which limited the opportunity of crystal growth for the PP matrix. This phenomenon indicates that the nanometal did not act as a nucleating agent [1].

Interestingly, silver zeolite exerted little acceleration on the crystallization of PP composite fibers when used at the lower concentration of 1%, but a greater zeolite amount of 2% caused a decrease of the fiber degree of crystallinity to 40.9%.

3.2. Mechanical Properties

The mechanical properties of a composite fiber are the most crucial features that remain difficult to predict because of the complex dependence on many factors. Molecular orientation and the degree of crystallinity are some important factors that affect the tensile properties.

The mechanical properties of the fibers, such as tensile strength, elongation-at-break, strain, fiber modulus and fiber tenacity, as well as denier were measured to evaluate the effect of the filler, take-up speed and draw ratio on the polymer fibers. Initially we used small amounts of silver (Table 2) and zinc (Table 4) to produce composite fibers at higher take-up speeds of 810 m/min with a draw ratio of 4.05. In the case of PP/0.5% Zn and PP/1% Zn (see Table 4) the yarns were produced at a lower take-up speed of 620 m/min and draw ratio of 2.07 to see its effect on the physical properties. The highest tenacity of 4.0 ± 0.12 g/denier and the lowest tenacity of 3.65 ± 0.23 g/denier were obtained for the set of PP fibers drawn at the draw of 4.0.

Generally, the mechanical properties of composite fibers were not significantly affected as the weight percentage of silver increased to 0.1%; and the values of tenacity, elongation, initial modulus and elongation-at-break were nearly maintained after compounding with silver particles. Surprisingly, fibers containing less than 0.1% zinc had a higher modulus and elongation-at-break indicating strong composite formation. Such a behavior implies that zinc nanoparticles could be used a processing aid in PP melt spinning. PP/1% silver zeolite composite fibers did not show any significant change in the tensile properties.

On the other hand, fiber tenacity decreased as the amount of silver or zinc content increased to 1.0% (Tables 3 and 4). This effect was also caused by a lower take-up

Table 3.
Mechanical properties of fibers containing silver nanoparticles

Sample*	Denier	Strain-at-break (%)	Fiber modules (gf/denier)	Fiber tenacity (gf/denier)	SD for fiber tenacity (gf/denier)
PP control	400	170.0	20.7	2.8	0.08
PP/1% Ag	400	145.7	22.9	2.4	0.12

* Draw ratio of 3.0. The yarn had 72 filaments.

Table 4.
Mechanical properties of polypropylene fibers containing zinc nanoparticles

Sample	Denier	Strain-at-break (%)	Fiber modulus (gf/denier)	Fiber tenacity (gf/denier)	SD for fiber tenacity (gf/denier)
PP control	410	68.3	34.6	3.65	0.26
PP/0.025% Zn	398	83.1	42.1	3.8	0.26
PP/0.05% Zn	399	90.8	43.5	3.9	0.10
PP/0.1% Zn	402	84.8	48.1	4.0	0.28
PP/0.5% Zn*	410	196.3	19.8	2.8	0.11
PP/1% Zn*	410	209.2	19.0	2.8	0.06

* Draw ratio of 2.07 and take-up speed of 620 m/min.

speed of 620 m/min and a lower draw ratio. The fiber elongation at break increased because during the test the fibers were not as oriented as those spun at higher draw ratios.

Generally, spinning performance measured by the number of broken filaments worsened with an increasing amount of nanometal. The mechanical properties of semi-crystalline polymers and particularly isotactic PP are mainly affected by their molecular weight, the nature of the crystal phase, such as α and β forms, the degree of crystallinity, spherulite size, the microstructure and the degree of molecular orientation in the direction of the fiber axis [23].

3.3. Real Filler Content and Antibacterial Efficacy

Table 5 shows the real nanometal content in PP fibers at various desired levels. Generally, the retention of silver and zinc nanoparticles was no more than 20% at low amounts of these metals for PP/0.5% Ag or PP/05% Zn compositions. Metal retention increased to 72.1, 85.9 and 88% in the case of PP/1% Ag, PP1% Zn and PP/1.5% Zn composite fibers, respectively. It was also observed that nanofillers agglomerated on screen filters at the filtration stage and also caused spinnability problems. This behavior was often observed when at least 1% nanometal was used. Frequent filament breaks were also documented at these high levels of silver or zinc particles. To solve for agglomeration particle problem, we propose the use of a powerful mixer for PP chips and nanometals prior to the extrusion process. In order

Table 5.
Real content of nanometals in PP fibers

Fiber composition	Fiber real metal content (%)	Metal retention (%)
PP/0.5% Ag	0.081	16.2
PP/1% Ag	0.721	72.1
PP/0.5% Zn	0.102	20.3
PP/1% Zn*	0.859	85.9
PP/1% Zn	0.601	60.1
PP/1.5% Zn	1.316	88.1

* Sample was produced with 0.2% of the non-ionic dispersing agent.

Table 6.
Antibacterial activity of PP/Ag fibers (plate count after 24 h in CFU/ml)

Fiber composition	Fiber real silver content (%)	*E. coli* count	Reduction *E. coli* (%)	*S. aureus* count	Reduction *S. aureus* (%)
PP control 1	Nil	1.26×10^8		9.16×10^4	
PP/0.1% Ag	0.028	1.46×10^7	88.4	1.75×10^4	80.9
PP control 2	Nil	5.62×10^5		1.632×10^3	
PP/0.5% Ag	0.081	5.24×10^4	90.7	–*	–*
PP/1% Ag**	0.721	5.24×10^4	99.99	1.73×10^2	89.4

* The analysis of *S. aureus* reduction for PP/0.5% was not determined.
** 99.99% reduction of *E. coli* in 1 h. The silver content was improved by addition of 0.2% of the non-ionic dispersing agent.

to reduce the loss of nanofillers during the melt extrusion of PP, a small amount of a nonionic dispersing agent (2 g/kg PP) was also incorporated. This facilitated better dispersion of the nanometal into the polymer matrix. Nanometal particles have large surface area and, therefore, can interact with proteins, affect cellular metabolism, and inhibit cell growth or the multiplication and growth of the bacteria and fungi. A noticeable improvement in antibacterial performance particularly for *E. coli* (Tables 6 and 7) for modified PP fibers was attained with a PP/0.5% Ag composite with real content of 0.081% Ag and also with a PP/0.5% Zn composite with 0.102% Zn. At a lower nanometal concentration, particularly for PP/0.1% Zn, these composite fibers exhibited only 20% bacterial reduction (Table 7). It is apparent from our data that a real metal content slightly higher than 0.1% is required to have a desirable antibacterial activity for silver and zinc nanoparticles.

It is clear from Table 6 that the percentage bacterial reduction of *E. coli* and *S. aureus* increased with an increase in nanometal content. A change of Ag content in PP fibers from 0.028 to 0.081% increased the percentage reduction of *E. coli*

Table 7.
Antibacterial activity of PP/Zn fibers

Fiber composition	Fiber real zinc content (%)	Reduction *E. coli* (%)		Reduction *S. aureus* (%)
		1 h	24 h	
PP control	Nil	20	20	Nil
PP/0.1% Zn	0.03	20	20	
PP/0.5% Zn	0.102	20	89	19.7
PP/1% Zn	0.601	99.99	99.99	91.4
PP/1.5% Zn	1.316	99.99	99.99	92.7

The reduction of *E. coli* after five washing of PP/Zn additives gave the same results as before washing.

from 88.4 to 90.7% and 99.99% for 0.721% Ag. Furthermore, an increase of silver content in PP fibers from 0.028 to 0.721% improved the percentage reduction of *S. aureus* from 80.9 to 89.4%.

In the case of the PP/0.5% Zn fiber composition containing 0.102% Zn, the reduction of *E. coli* reached 89% and 19.7% *for S. aureus*. A better antibacterial efficacy was observed for the PP/1% Zn fiber with 0.601% Zn as the bacterial reduction was 99.99% and 91.4% for *E. coli* and *S. aureus*, respectively (Table 7). At large zinc content of 1.316% a 99.99% reduction for *E. coli* and 92.6% for *S. aureus* was observed.

In summary, it is plausible to conclude that the antibacterial activity of the composite Ag and Zn fibers was comparable against *E. coli* and *S. aureus*.

The mechanistic aspect of the zinc antimicrobial efficacy remains an open issue. However, it is our belief that this will probably be an ionic mechanism. Recent studies [24, 25] prove that silver nanoparticles get oxidized in water and release silver ions. The ions form complexes with various compounds, proteins or DNA, leading to bacterial death [22]. It is well known that a protective layer of zinc oxide and carbonate is formed on zinc particle surfaces, so it is possible that the release of zinc ions can also occur. Zinc oxide is a well known deodorizing and antibacterial agent [25–28]. It is often used to treat diaper rashes and some other types of skin infections. We shall investigate the ionic mechanisms for zinc particles in a future publication.

3.4. Antistatic Properties

Depending on their position in the triboelectric series, polymers play a major role in the type of static charge formed [20]. Polyester and PP fibers accumulate negative charges, and nylon builds up positive charges after friction between the stainless steel charge pin (Fig. 3). Furthermore, based on our unpublished experimental results, PP had the lowest charge generation, when compared to nylon and polyester.

Table 8.
Electrostatic tests data for PP yarns with silver nanoparticles

Sample	First probe potential (V)	Second probe potential (V)	Calculated initial potential (V)	Decay time (s)
PP control	−1023	−855	−1041	1.25
PP/0.3% Ag	−347	−220	−348	0.51
PP/0.5% Ag	−175	−111	−213	0.16

PP/Ag composite fibers containing different concentrations of Ag proved to be antistatic when using the linear tester method (Table 8). Thus, the potential at the second probe was found to decrease from −855 V for PP control to −111 V for PP/0.5% Ag yarns. A dramatically shorter decay time was also documented for the latter yarn.

Since PP fibers containing silver particles showed improved antistatic properties, it can be expected that fibers with zinc or zinc oxide particles should show similar behavior. This research project will be a topic of our future publication.

3.5. Fiber Surface Observations

Melt-spun PP fibers having a round cross-section usually have smooth surfaces and no unusual morphological features can be expected. Indeed, as can be seen from Fig. 10a, our fibers without any metal additives exhibited this feature.

However, the surface of the composite fibers was very unique. A few large agglomerates of 400 or 675 nm and many smaller ones having the size around 135 nm were observed on the fibers containing 0.72% silver (Fig. 10b and 10c). Nanoparticles of 70 nm can be also seen. Most of these particles were imbedded in the polymer surface with larger agglomerates clearly visible on the fiber surface.

Typical FESEM images of PP fibers with 0.56% zinc are given in Fig. 10d and 10e. Larger aggregates having size from 149 to 457 nm (Fig. 10d) and 133 to 457 nm (Fig. 10e) were documented. Surface of zinc composites fibers was not as smooth as for the control PP fibers.

In fact, this study revealed that some of the silver and zinc nanoparticles had agglomerated into irregular clusters because of attractive interactive forces on fiber surface. Furthermore, it showed that blending of polypropylene with silver or zinc nanoparticles with the aid of a non-nionic surfactant can produce unique particle distribution on the fiber surface. Obviously, having nanoaggregates on fiber surfaces could be very beneficial for the development of antibacterial non-woven products.

We also believe that a twin screw extruder could also be used to produce a concentrate of these nanoparticles prior to compounding with polypropylene. Such an approach should assure a good dispersion of these additives in polypropylene and improve fiber properties. A degree of particle aggregation could be therefore re-

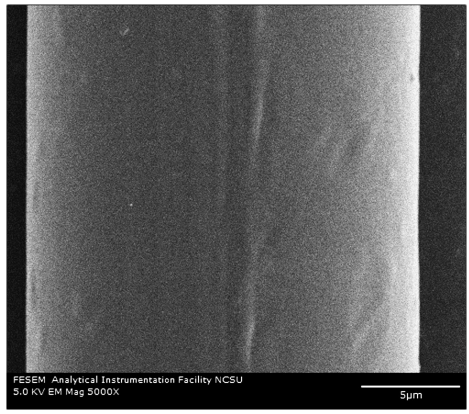

(a)

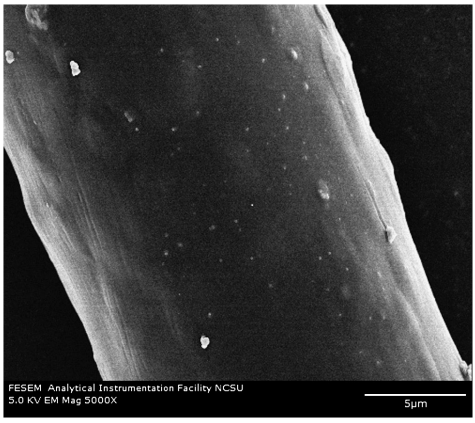

(b)

(c)

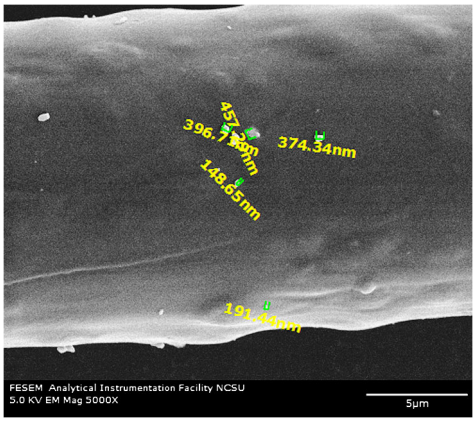

(d)

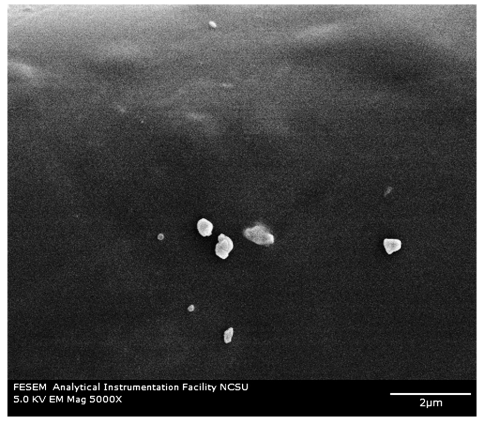

(e)

Figure 10. FESEM images of (a) PP fiber and PP fibers with (b, c) 0.72% Ag and (d, e) 0.56% Zn. This figure is published in colour in the online edition of this journal, which can be accessed *via* http://www.brill.nl/jbs

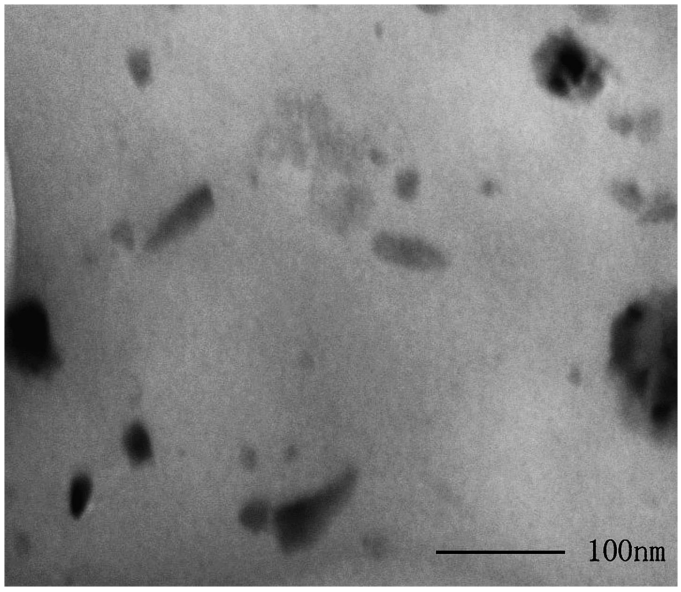

Figure 11. TEM micrograph of PP/1.0 wt% Ag nanocomposites. Reprinted with permission from e-Polymers [29].

duced and lower amount amounts of additives could be used to assure a satisfactory antibacterial efficacy.

3.6. Fiber Cross-section Observations

Melt processing of PP with silver nanoparticles does not always result in a fine distribution of these species. Furthermore, the particle shape may change as a result of a high shear rate used in the process. Colloidal silver particles are round but during PP melt spinning or some other type of processing nanoparticles could agglomerate into clusters of various sizes and shapes (see for example Fig. 11, taken with permission from Ref. [29]).

Our observations on silver PP composite fibers confirm that the silver nanoparticles formed clusters of various shapes and sizes. The silver cluster size varied from 113 to 562 nm (Fig. 12). The smallest particle of 113 nm can be seen in Fig. 12b. Interestingly, a large silver aggregate of 562 nm (Fig. 12c) consisted of a number of smaller particles and had a very irregular shape.

Zinc nanoparticles also formed the clusters; however, the shape of these aggregates was more uniform. The smallest particles size was 250 nm (Fig. 13a) and the largest aggregate of 567 nm was observed in Fig. 13c. As mentioned before, the use of a high shear rate could be used to break these large particles.

4. Conclusions

Antibacterial efficacy of PP fibers increased with an increasing real filler content. It can be concluded that real silver content in PP fibers has to be more than 0.081%

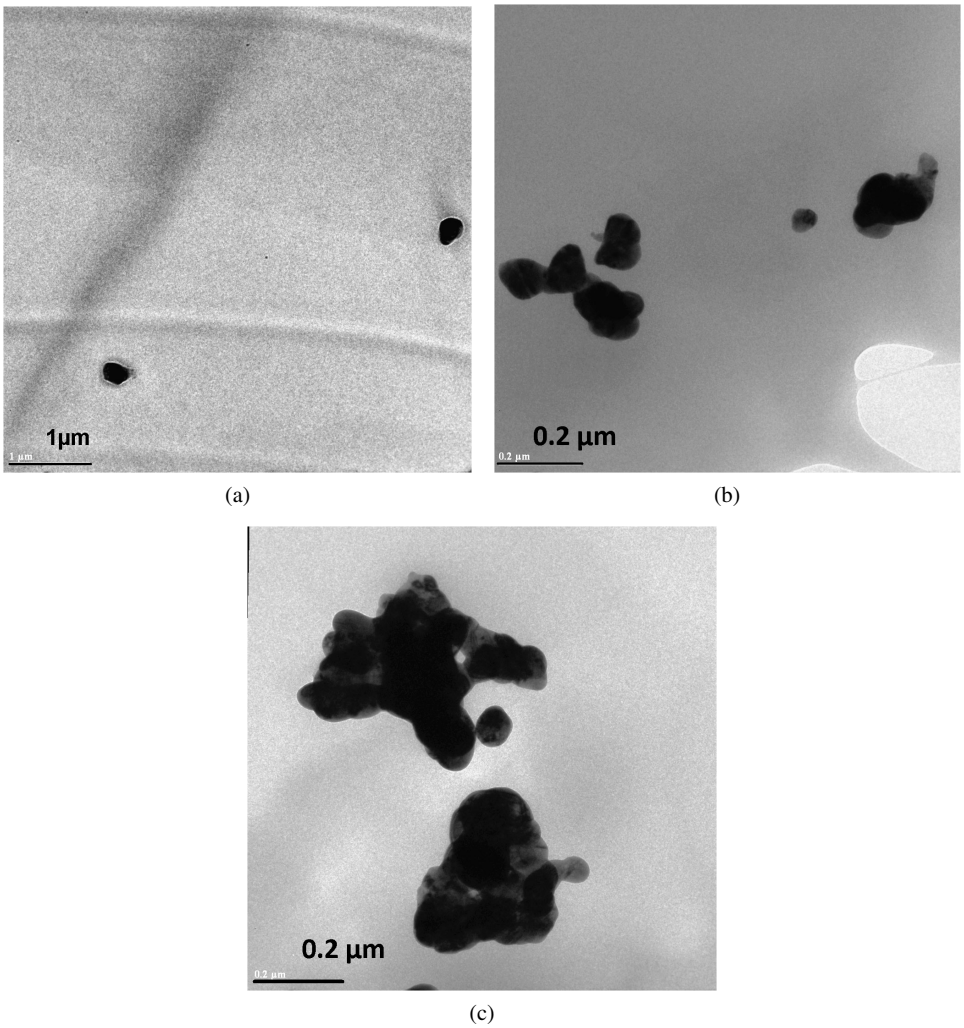

(a) (b)

(c)

Figure 12. TEM images of PP fibers with 0.72% Ag.

and zinc filler content has to be more than 0.102% to see significant *E. coli* or *S. aureus* reduction. Excellent *E. coli* reduction was observed with 0.6% zinc and 0.72% silver filler content. The most effective amount of zinc particles should be optimized.

This study demonstrates that various antibacterial, textile non-woven products can be produced by melt-spinning PP with metal nanoparticles. However, dispersion of a small amount of less expensive zinc or zinc oxide particles is a challenging issue. The use of a twin screw extruder should assure good mixing and reduce particle agglomeration while making larger batches of this blend. A non-nionic dispersing agent should be also beneficial to try. This approach should bring the critical amount of zinc to a much lower level.

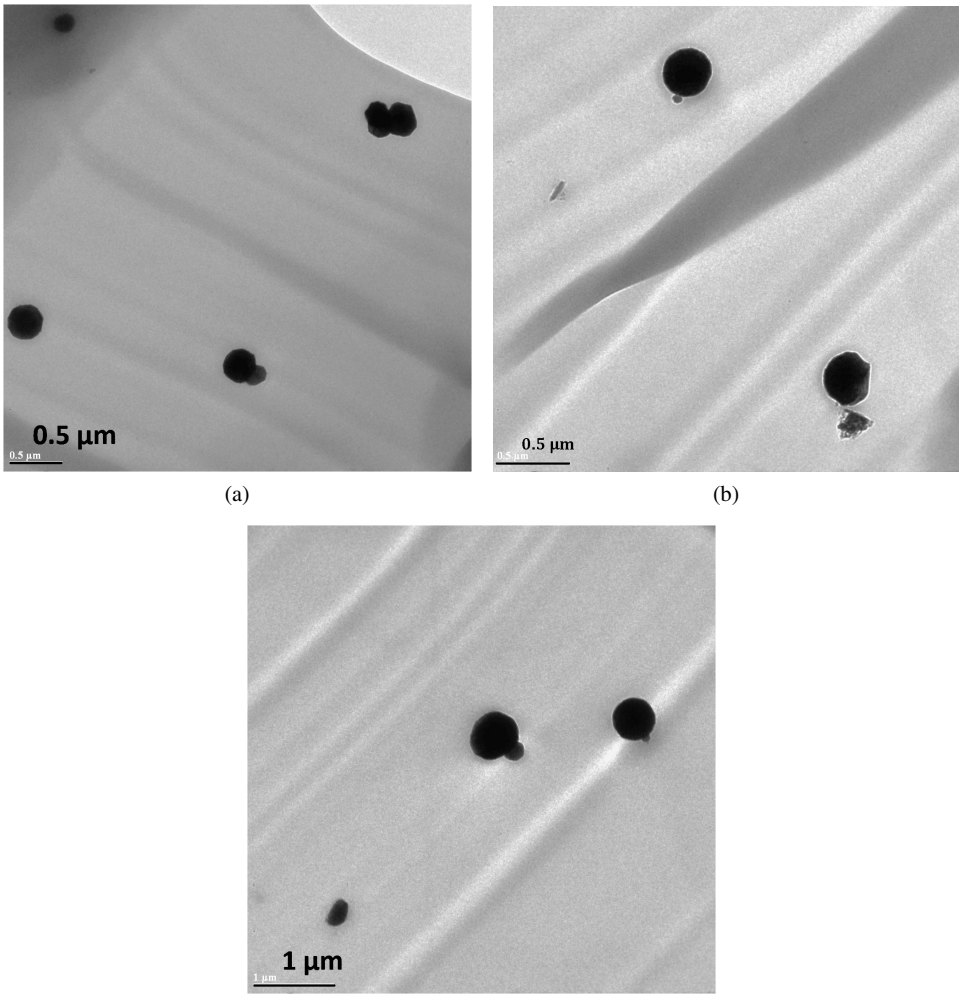

(a) (b)

(c)

Figure 13. TEM images of PP fibers with 0.56% Zn.

Since PP fibers containing silver particles showed improved antistatic properties, it can be expected that the fibers with zinc particles should show similar behavior. This research project will be a topic of our future publication.

Acknowledgements

The authors gratefully acknowledge the backing of the National Science Foundation (Contract NSF Int. 0809520) and the US Department of State for supporting this research under the USA-Egypt Science and Technology Development Fund (STDF project No 434). We thank Ms. Lindsay Zielinske, a researcher assistant at AEGIS Environments for the antibacterial analysis. Ms Kimberly Hutchison, man-

ager at the Soil Department, NCSU is appreciated for metals content analysis. The authors would also like to thank the following colleagues from the College of Textiles at North Carolina State University namely Mr. Timothy Mumford, manager of the melt extrusion laboratory, Ms Teresa White, manager of the Physical Testing Laboratory and Ms Brigit Anderson, manager of the Analytical Laboratory. We greatly appreciate useful reviewer's comments that were included in this paper.

References

1. S. H. Jeong, S. Y. Yeo and S. C. Yi, *J. Mater. Sci.* **40**, 5407 (2005).
2. S. Y. Yeo, H. J. Lee and S. H. Jeong, *J. Mater. Sci.* **38**, 2143 (2003).
3. X. Chen and H. J. Schluesener, *Toxicol. Lett.* **176**, 1 (2008).
4. R. Purwar and M. Joshi, *AATCC Rev.*, 22 (March 2004).
5. J. F. Williams, *AATCC Rev.*, 17 (April 2005).
6. L. Qian, *AATCC Rev.*, 14 (May 2004).
7. C. Radheshkmar and H. Munstedt, *React. Funct. Polym.* **66**, 780 (2006).
8. R. Dastjerdi, M. R. M. Mojtahedi and A. M. Shoshtari, *Fibers Polym.* **9**, 727 (2008).
9. J. Broda, A. Gawlowski, C. Slusarczyk, A. Wlochowicz and J. Fabia, *Dyes Pigments* **74**, 508 (2007).
10. M. Joshi, M. Shaw and B. S. Butola, *Fibers Polym.* **5**, 59 (2004).
11. S. Houshyar, R. A. Shanks and A. Hodzic, *J. Appl. Polym. Sci.* **96**, 2260 (2005).
12. D. W. Chae, K. B. Shim and B. C. Kim, *J. Appl. Polym. Sci.* **109**, 2942 (2008).
13. M. Afshari, R. Kotek, B. S. Gupta, H. Kish and H. N. Dast, *J. Appl. Polym. Sci.* **97**, 532 (2005).
14. S. M. Abo El-Ola, R. Kotek, M. King, J. H. Kim, R. Monticello and J. A. Reeve, *J. Biomater. Sci. Polymer Edn* **15**, 1545 (2004).
15. S. Base, *Polymer* **48**, 356 (2007).
16. J. Brandrup and E. H. Immergut, *Polymer Handbook*, 2nd edn. Wiley, New York, NY (1999).
17. *AATCC Technical Manual*. American Association of Textile Chemists & Colorists, Research Triangle Park, NC (2001).
18. F. Wendler, F. Meister, R. Montigny and M. Wagener, *Fibers Textiles East. Eur.* **15**, 64 (2007).
19. A. M. Seyam, Y. Cai and W. Oxenham, *J. Textile Inst.* **1**, 1 (2008).
20. J. E. Mark, *Polymer Data Handbook*. Oxford University Press, Oxford (1999).
21. N. Gomez, R. Julia, P. Erra and A. Naik, *Textile Res. J.* **64**, 648 (1994).
22. C. Radheshkumar and H. Munstedt, *Mater. Lett.* **50**, 1949 (2005).
23. P. Tordjeman, C. Robert and P. Gerard, *The Mechanical Properties of α,β-Polypropylene*, presented at Materiaux 2002, Tours, October 21–25 (2002).
24. C. Damm, H. Münstedt and A. Rösch, *Mater. Chem. Phys.* **108**, 61 (2008).
25. J. S. Hoskins, T. Karanfil and S. M. Serkiz, *Environ. Sci. Technol.* **36**, 784 (2002).
26. D. Boyd, H. Li, D. A. Tanner, M. R. Towler and J. G. Wall, *J. Mater. Sci. Mater. Med.* **17**, 489 (2006).
27. R. Dastjerdi, M. R. M. Mojtahedi, A. M. Shoshtari, A. Khosroshahi and A. J. Moayed, *Textile Res. J.* **79**, 1099 (2009).
28. A. Yadav, V. Prasad, A. A. Kathe, S. Raj, D. Yadav, C. Sundaramoorthy and N. Vigneshwaran, *Bull. Mater. Sci.* **29**, 641 (2006).
29. S. C. Tjong and S. Bao, *e-Polymers* **139**, 1 (2007).